

## Orientational epitaxy of van der Waals molecular heterostructures

Guo, Lu'an; Guo, Quanmin; Wang, Yitao; Kaya, Dogan; Palmer, Richard; Chen, Guangde

DOI:

[10.1021/acs.nanolett.8b02238](https://doi.org/10.1021/acs.nanolett.8b02238)

License:

None: All rights reserved

*Document Version*

Peer reviewed version

*Citation for published version (Harvard):*

Guo, L, Guo, Q, Wang, Y, Kaya, D, Palmer, R & Chen, G 2018, 'Orientational epitaxy of van der Waals molecular heterostructures', *Nano Letters*, vol. 18, pp. 5257-5261. <https://doi.org/10.1021/acs.nanolett.8b02238>

[Link to publication on Research at Birmingham portal](#)

### **Publisher Rights Statement:**

Final Version of Record available at: <https://dx.doi.org/10.1021/acs.nanolett.8b02238>

### **General rights**

Unless a licence is specified above, all rights (including copyright and moral rights) in this document are retained by the authors and/or the copyright holders. The express permission of the copyright holder must be obtained for any use of this material other than for purposes permitted by law.

- Users may freely distribute the URL that is used to identify this publication.
- Users may download and/or print one copy of the publication from the University of Birmingham research portal for the purpose of private study or non-commercial research.
- User may use extracts from the document in line with the concept of 'fair dealing' under the Copyright, Designs and Patents Act 1988 (?)
- Users may not further distribute the material nor use it for the purposes of commercial gain.

Where a licence is displayed above, please note the terms and conditions of the licence govern your use of this document.

When citing, please reference the published version.

### **Take down policy**

While the University of Birmingham exercises care and attention in making items available there are rare occasions when an item has been uploaded in error or has been deemed to be commercially or otherwise sensitive.

If you believe that this is the case for this document, please contact [UBIRA@lists.bham.ac.uk](mailto:UBIRA@lists.bham.ac.uk) providing details and we will remove access to the work immediately and investigate.

# Orientational Epitaxy of Van der Waals Molecular Heterostructures

Lu'an Guo,<sup>#§</sup> Yitao Wang,<sup>§</sup> Dogan Kaya,<sup>¶</sup> Richard E Palmer,<sup>§</sup> Guangde Chen<sup>#</sup> and Quanmin Guo<sup>§\*</sup>

<sup>#</sup> *Department of Applied Physics and Key Laboratory for Quantum Information and Quantum Optoelectronic Devices of Shaanxi Province, Xi'an Jiaotong University, Xi'an 710049, China*

<sup>§</sup> *School of Physics and Astronomy, University of Birmingham  
Edgbaston, Birmingham, B15 2TT, UK*

<sup>¶</sup> *Department of Electronics and Automation, Vocational School of Adana, Cukurova University, 01160, Cukurova, Adana, Turkey*

<sup>§</sup> *College of Engineering, Swansea University, Bay Campus, Fabian Way, Swansea, SA1 8EN, UK*

**ABSTRACT:** The shape of individual building blocks is an important parameter in bottom-up self-assembly of nanostructured materials. A simple shape change from sphere to spheroid can significantly affect the assembly process due to the modification to the orientational degrees of freedom. When a layer of spheres is placed upon a layer of spheroids, the strain at the interface can be minimised by the spheroid taking a special orientation.  $C_{70}$  fullerenes represent the smallest spheroids and their interaction with a sphere-like  $C_{60}$  is investigated. We find that the orientation of the  $C_{70}$  within a close-packed  $C_{70}$  layer can be steered by contacting a layer of  $C_{60}$ . This orientational steering phenomenon is potentially useful for epitaxial growth of multilayer van der Waals molecular heterostructures.

**Key words:** Van der Waals heterostructures; Epitaxy; Self-assembly; fullerene; graphene; interface; scanning tunnelling microscopy.

Epitaxial growth of thin films, a process extensively used in the semiconductor industry for fabricating electronic and optoelectronic devices,<sup>1-4</sup> has recently found applications in a number of emerging fields such as Van der Waals heterostructures,<sup>5-7</sup> metal organic frameworks (MOFs),<sup>8</sup> organic semiconductors<sup>9,10</sup> and colloidal assembly.<sup>11,12</sup> In a typical heteroepitaxy process, a thin film of element A is grown on a crystalline substrate of element B. The thin film of A is normally under some stress which arises from lattice mismatch between the two elements,<sup>13</sup> and consequently, there has been much interest in fabricating strained layers by deliberately introducing stress into the grown layers.<sup>14-16</sup> The structure of the interface depends not only on the lattice mismatch, but also on the type of bonding involved.<sup>17</sup> For van der Waals epitaxy<sup>17</sup> where a layered material grows on top of another layered material such as the stacking of transition metal dichalcogenides ( $MoS_2$ ,  $WSe_2$ , etc.), multilayer stacks of high quality 2D materials can be formed in the presence of very large lattice mismatch.<sup>17</sup> For such 2D materials, the formation of an epitaxial layer is mainly controlled by the strong atomic bonding within the layer, with the weak van der Waals interaction between the layers playing a much less significant role.

The term "van der Waals epitaxy" should not be restricted to the epitaxial growth of the conventional van der Waals heterostructures.<sup>5-7</sup> By introducing organic molecules for example, hybrid organic/inorganic van der Waals heterostructures have been made.<sup>18</sup> The self-assembly of organic molecules on top of 2D materials opens up new avenues for fabricating hybrid functional materials.<sup>18</sup> Layered materials can also be produced by stacking organic molecules based completely on van der Waals interactions. One can take the layer-by-layer approach<sup>19</sup> to synthesize a molecular material consisting of alternating layers of two molecules (A and B). Molecules within both the A and B layers are bonded via van der Waals interaction. The bonding

between the A and B layers is also van der Waals in nature. Without any specific interaction such as hydrogen bonding or ionic bonding, controlling the interfacial structure between two van der Waals molecular layers can be a real challenge. Here we investigate the structure of the  $C_{60}/C_{70}$  interface. By depositing  $C_{60}$  and  $C_{70}$  sequentially onto highly oriented pyrolytic graphite (HOPG) at room temperature, a van der Waals bilayer is produced. There are two interesting aspects of this bi-layer system. i) both molecules are significantly larger than typical atoms, but much smaller than colloidal particles. The system serves as a good example to understand size scalability in nucleation and growth.<sup>20</sup> ii) The different shapes of the two molecules offer a good example to study the packing of objects with different geometric forms.<sup>21,22</sup>

$C_{60}$  is a useful component in organic solar cells<sup>23,24</sup> and in molecular p-n hetero-junctions.<sup>10</sup> When combined with gold atoms,  $C_{60}$  molecules are able to assemble into hybrid magic number clusters<sup>25,26</sup> or nano-rings.<sup>27</sup> The assembly of  $C_{60}$  on various atomically flat solid substrates has been extensively studied.<sup>28-35</sup> It has been found that  $C_{60}$  molecules have strong tendency to form close-packed layers and do so on many solid surfaces where the molecule-substrate interaction is relatively weak. Investigations of  $C_{60}$  and  $C_{70}$  mixture have found several bulk phases of the  $(C_{60})_x(C_{70})_y$  alloy and a miscibility gap.<sup>36-37</sup> The mixing of these two molecules has also been studied using high-resolution scanning tunnelling microscopy (STM).<sup>38,39</sup> The direct interaction between a close-packed  $C_{60}$  layer with a  $C_{70}$  layer has not been studied so far. Due to the different lattice parameters, a  $C_{60}$ - $C_{70}$  bilayer is expected to be strained with tensile stress in the  $C_{60}$  layer and compressive stress in the  $C_{70}$  layer. How does the bilayer accommodate the strain is an interesting problem. In addition to the usual ways of strain relieve such as the introduction of dislocations, the  $C_{70}$  molecule has a property that atoms do not have. The  $C_{70}$  molecule can take at least two different orientations: i) with the long axis perpendicular to the interface or ii) with the long axis parallel to the interface. This extra degrees of freedom in molecular orientation provides additional channels for strain relieve at the interface. Here we report findings on the orientational switching of the  $C_{70}$  molecule and the detailed structure of the  $C_{60}$ - $C_{70}$  interface.

Figure 1a shows an STM image acquired from a region of the HOPG sample covered by a monolayer of molecules. The sample was prepared by sequentially deposition of 1.2 monolayers (ML) of  $C_{70}$  and 0.2 ML of  $C_{60}$  at RT. It was then annealed at 425 K for 30 minutes to initiate some mixing of the two molecules. Parts of the substrate are covered by multiplayers. Here we concentrate on this particular region where a  $C_{60}$ -rich layer (single layer) sits next to a  $C_{70}$ -rich layer (single layer), with both the  $C_{60}$ -rich and the  $C_{70}$ -rich layers sitting directly above the HOPG substrate. The direction of close-packed molecules is the same for both  $C_{60}$  and  $C_{70}$  in this image. This may arise from some specific interactions at the  $C_{60}$  and  $C_{70}$  boundary. In Fig. 1a, the distance defined by the two parallel yellow lines accommodates 14 rows of  $C_{70}$  and 15

rows of  $C_{60}$ . Thus the ratio of the nearest neighbor  $C_{70}$ - $C_{70}$  distance to that of the  $C_{60}$ - $C_{60}$  distance is 1.07. Taking the nearest neighbor  $C_{60}$ - $C_{60}$  distance as 1.0 nm,<sup>40</sup> the nearest neighbor  $C_{70}$ - $C_{70}$  distance is found to be 1.07 nm. These values are in good agreement with those found in the bulk fullerenes using x-ray diffraction (XRD),<sup>41</sup> indicating that the structure of the monolayer fullerenes on HOPG is very close to the bulk projection of the (111) plane of the corresponding fullerite.

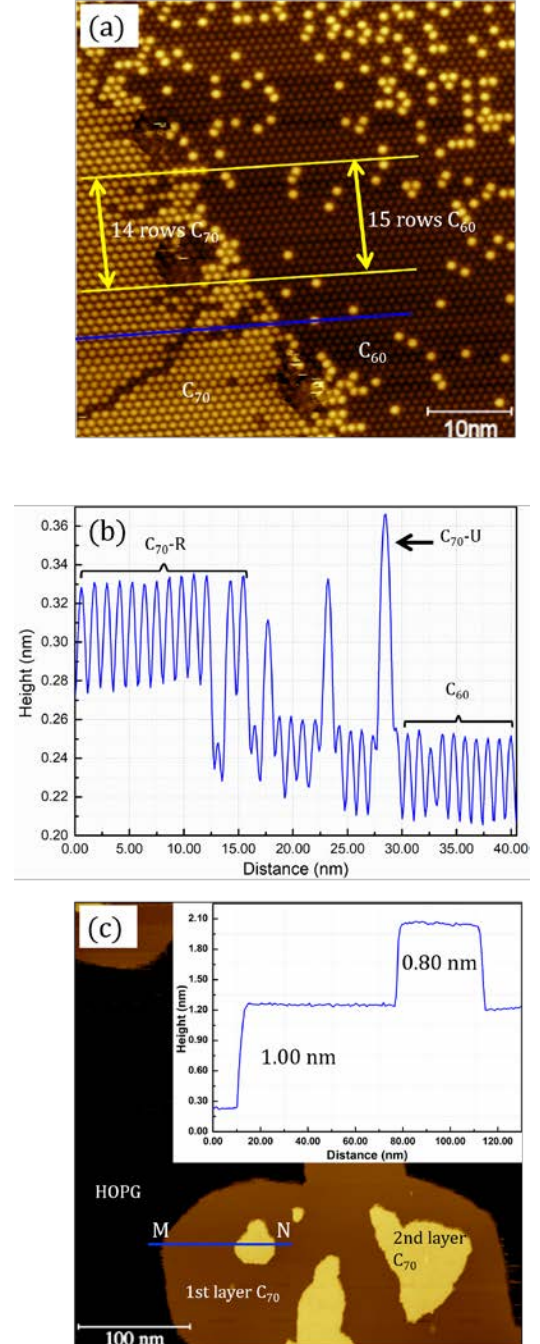
The crystalline  $C_{70}$  has an fcc structure at temperatures above 340 K. In this fcc phase, the  $C_{70}$  molecule rotates freely with no orientational order. The nearest neighbor distance in the fcc phase is 1.06 nm.<sup>41</sup> Below 340 K, a phase transition occurs such that the long axis of the  $C_{70}$  molecule becomes frozen in the direction perpendicular to one of the close-packed layers. As a consequence, the in-plane nearest neighbor  $C_{70}$ - $C_{70}$  distance is reduced from 1.06 nm to 1.01 nm. The 1.07 nm nearest neighbor  $C_{70}$ - $C_{70}$  distance measured by our STM is a good indication that the  $C_{70}$  molecules within the first  $C_{70}$  layer on HOPG is rotationally disordered even at RT.

Figure 1b displays the height profile along the blue line in Fig. 1a. In this profile, the tallest feature ( $C_{70}$ -U, U for upright), 0.11 nm taller than  $C_{60}$ , corresponds to an isolated  $C_{70}$  molecule trapped inside the  $C_{60}$ -rich domain. In Fig 1a, there are approximately 1% of  $C_{60}$  molecules within the  $C_{60}$ -rich domain substituted by trapped  $C_{70}$  molecules. The trapped  $C_{70}$  occupies the space vacated by a  $C_{60}$  molecule. Due to steric hindrance, the trapped  $C_{70}$  can only take an orientation with its long axis perpendicular to the substrate. By having the long axis perpendicular to the substrate, a trapped  $C_{70}$  molecule inside the  $C_{60}$  domain has the same footprint as a  $C_{60}$ . This is a favorable configuration because of the nearly zero strain introduced into the  $C_{60}$  lattice by substituting a  $C_{60}$  with a  $C_{70}$  in such a manner. The 0.11 nm height difference between the trapped  $C_{70}$  and the  $C_{60}$  molecules is consistent with this conclusion. Height measured by STM has electronic contributions as well as geometric contributions, and it is not always straightforward to separate the two contributions. The height profile shown in Fig. 1b is independent of the bias voltage, suggesting mainly a geometric contribution. Moreover, charge transfer between HOPG and the fullerenes is expected to be weak, making any electronic contribution to the height measurement insignificant.

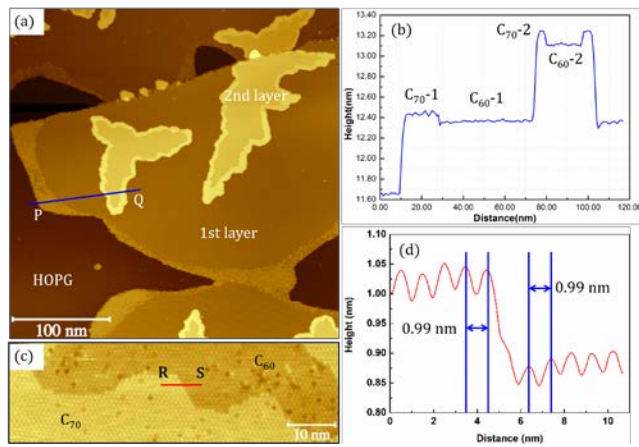
The  $C_{70}$  molecules inside the  $C_{70}$ -rich domain ( $C_{70}$ -R, R for rotation) appear lower than the trapped  $C_{70}$  molecules by 0.04 nm. This is because the molecules inside the closed-packed  $C_{70}$  domain do not have a fixed orientation. They are under constant rotation. When a free-rotating  $C_{70}$  is being imaged by the STM, it can be regarded as spending part of its time with the long axis perpendicular to the substrate and the rest of the time with the long axis parallel to the substrate. With the molecular rotation taking place at a much faster rate than the response time of the STM tip, an effective tunnel current is registered. If the tip height is fixed, the effective tunnel current would be lower when the tip is above a rotating  $C_{70}$  molecule than when it is above an upright  $C_{70}$  molecule.

Figure 1c shows an STM image acquired from the HOPG sample after 1.2 ML of  $C_{70}$  is deposited at RT. The second molecular layer is formed before the first layer is completed. The inset in Fig. 1c shows a height profile measured along the blue line M-N. Based on this height profile, the first layer measured from the HOPG surface is 1.00 nm tall. The second layer is 0.80 nm above the first layer. The ratio of 1.00/0.80 is consistent with two layers of close-packed hard spheres with the second layer spheres sitting in the three fold hollow site of the first layer. For

$C_{60}$  on HOPG, the first layer is 0.80 nm above the HOPG substrate, and the second  $C_{60}$  layer is 0.70 nm above the first layer.



**Figure 1.** (a) STM image acquired at RT from HOPG covered by a single layer of  $C_{60}/C_{70}$ . There is a  $C_{70}$ -rich domain to the left and a  $C_{60}$ -rich domain to the right of the image. The bright features inside the  $C_{60}$  domain are trapped  $C_{70}$  molecules.  $C_{60}$  molecules inside the  $C_{70}$ -rich domain seem to have aggregated into zig-zag rows. (b) Height profile along the blue line in (a). (c) Layers of  $C_{70}$  on HOPG following RT deposition. The 2<sup>nd</sup> layer forms before the first layer is completed. Inset is the height profile measured along line M-N.



**Figure 2.** (a) STM image of the sample after 0.2 ML of  $C_{70}$  are added to a pre-existing 1.2 ML  $C_{60}$  at RT. The post-deposited  $C_{70}$  form rims around the preformed  $C_{60}$  islands. (b) Height profile along line P-Q in (a). Characteristic heights corresponding to the first layer  $C_{60}$  ( $C_{60-1}$ ), first layer  $C_{70}$  ( $C_{70-1}$ ), second layer  $C_{60}$  ( $C_{60-2}$ ) and second layer  $C_{70}$  ( $C_{70-2}$ ), respectively, are clearly identified. (c) STM image showing a boundary between  $C_{60}$  and  $C_{70}$  in the second layer. (d) Height profile along line R-S in (c).

Figure 2a shows an STM image from the sample after adding 0.2 ML of  $C_{70}$  molecules onto the HOPG with a pre-existing 1.2 ML of  $C_{60}$ . The  $C_{70}$  molecules are found to attach to the edges of the pre-formed  $C_{60}$  islands in both the first and the second layers. The second layer  $C_{60}$  has the same lattice parameter as the first layer. However, the second layer  $C_{70}$  has a smaller lattice parameter than  $C_{70}$  in the first layer. Fig. 2c shows a boundary between the second layer  $C_{60}$  and the second layer  $C_{70}$ . This boundary is noticeable mainly because of the height difference between the two molecules. The  $C_{70}$  domain merges seamlessly with the neighbouring  $C_{60}$  domain without the presence of any dislocations at the boundary. Therefore, the second layer  $C_{70}$  is lattice-matched with the underlying  $C_{60}$  layer, and this can only be achieved if the  $C_{70}$  molecules take the upright configuration with their long axis perpendicular to the surface. The  $C_{60}$ - $C_{70}$  boundary in the second layer is sharp with no signs of inter-mixing. This suggests a rigid island boundary for the second layer  $C_{60}$ . The  $C_{70}$  rim in the first layer has  $C_{60}$  molecules incorporated. This is because the island edges of the first layer  $C_{60}$  are rather “fluidic” at RT and there exists a two-dimensional vapor-like  $C_{60}$  phase in the vicinity of the  $C_{60}$  islands. Post deposited  $C_{70}$  are thus able to mix with the  $C_{60}$  “vapor” before condensing into the rim. From the data shown in Fig. 2, we can conclude that the first layer  $C_{60}$  has a steering effect on the orientation of the  $C_{70}$  molecules sitting directly above. The  $C_{70}$  molecules stand upright with their long axis perpendicular to the substrate. As a consequence, the second layer  $C_{70}$  has an excellent lattice match with the  $C_{60}$  layer below. Figure 3a shows a schematic diagram illustrating how the second layer  $C_{70}$  molecules form lattice-matched structure with  $C_{60}$ . Fig. 3b indicates a possible structure if  $C_{60}$  molecules are post-deposited onto an existing  $C_{70}$  layer if all  $C_{70}$  molecules have the same upright orientation.

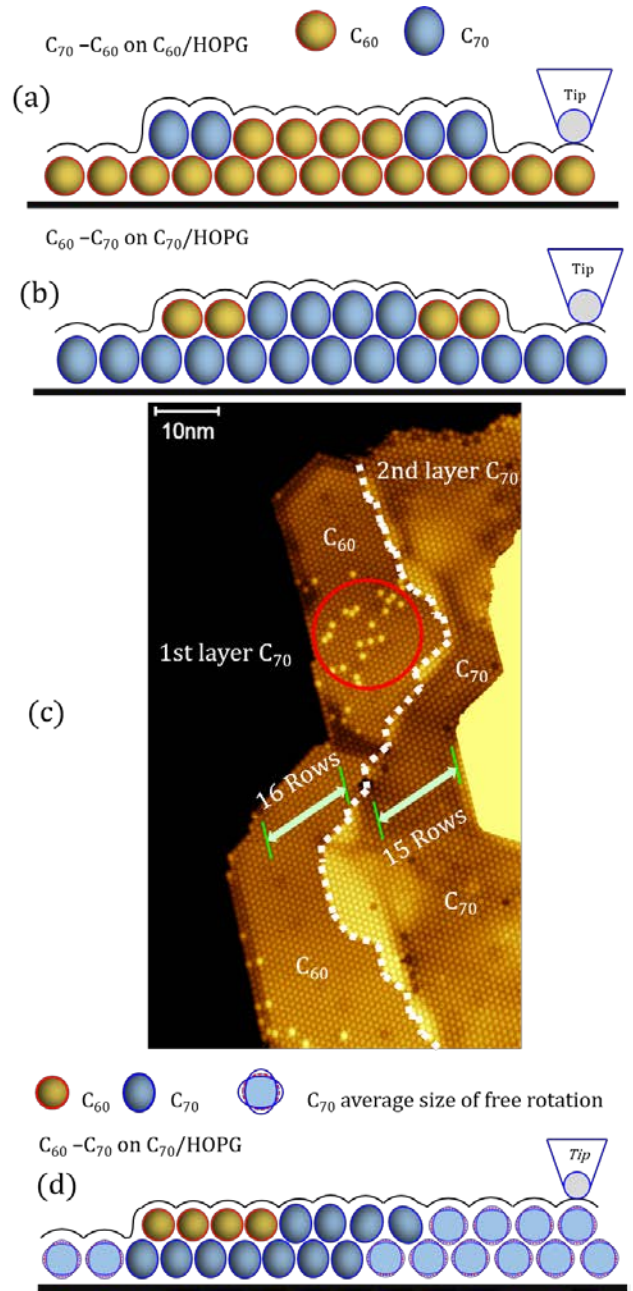


**Figure 3.** (a) Schematic of the tall  $C_{70}$  rim formed around a  $C_{60}$  island in the second layer. (b) A possible structure of a short  $C_{60}$  rim formed around a second layer  $C_{70}$  island. (c) STM image showing two interconnecting  $C_{60}$  and  $C_{70}$  domains in the second layer. They both sit on a first layer  $C_{70}$ . Following the deposition of  $C_{60}$ , the sample was annealed to 425 K for 30 minutes. Dashed lines highlight the boundary between  $C_{60}$  and  $C_{70}$ . Some scattered  $C_{70}$  molecules possibly due to the effect of annealing at 425 K, highlighted by the red circle, are observed within the  $C_{60}$  domain. The  $C_{60}$  and  $C_{70}$  domains can be distinguished by their different lattice parameters, rather their heights. (d) Proposed structural model for the interface between first layer  $C_{70}$  and the second layer  $C_{60}$ .

Fig. 3c is an STM image from the sample after 0.2 ML  $C_{60}$  molecules are deposited onto a preformed 1.2 ML  $C_{70}$ . The image



is displayed with enhanced contrast to compare the second layer  $C_{60}$  and  $C_{70}$ . The first layer  $C_{70}$  can be seen in the original image but not visible in this processed image. The boundary between  $C_{60}$  and  $C_{70}$  in the second layer can be identified by a narrow region of uneven height contrast, highlighted with dashed lines. The  $C_{60}$  molecules appear to have the same height as  $C_{70}$  molecules in the second layer. However, the  $C_{60}$  domain has a smaller lattice parameter. As can be seen in Fig. 3c, within the distance covered by the length of the double-headed arrows, there are 16 rows of  $C_{60}$  within the  $C_{60}$  domain. The same distance is occupied by 15 rows of  $C_{70}$  molecules inside the  $C_{70}$  domain. This 16/15 ratio is roughly the same, subject to experimental error, as that found from Fig. 1 for the first layer molecules. We have repeated such measurement in different areas of the sample and found a consistent value for this ratio. The schematic diagram in Fig. 3d is used to explain the characteristics in Fig. 3c. We already know that  $C_{70}$  molecules in the first layer have complete freedom of rotation. When  $C_{60}$  molecules are added on top of the  $C_{70}$  first layer, the  $C_{60}$  molecules can choose either to sit in the hollow site and form a strained layer under tensile stress, or to form a strain-free layer by forcing the first layer  $C_{70}$  to stand upright. Our data indicates that the second layer  $C_{60}$  has formed a nearly strain-free layer. We cannot claim that there is absolutely zero strain although any residual strain is expected to be insignificantly low. This post-formed second layer  $C_{60}$  thus forces the underlying  $C_{70}$  to stand upright leading to a lattice-matched interface. The interaction between the second layer  $C_{70}$  and the first layer  $C_{70}$ , on the other hand, does not help to improve the orientational ordering.  $C_{70}$  molecules in both the first and second layers are in their free rotating state. The height of two layers of free-rotating  $C_{70}$  molecules is comparable to the height of a  $C_{60}$  layer standing above a  $C_{70}$  layer with the upright orientation. From the data shown in Fig. 1, we find that the upright  $C_{70}$  molecules are taller than the rotating molecules by 0.04 nm. This makes the height of  $C_{60}+C_{70}$ -U 1.70 nm, and the height of two layers of  $C_{70}$ -R 1.72 nm. Along the  $C_{60}$ - $C_{70}$  boundary, there are a small number of tall  $C_{70}$  molecules. Thus along the boundary, some  $C_{70}$  molecules are approximately standing upright. As can be seen in Fig. 3c, this transition region at the boundary does not appear to have any long-range order.  $C_{60}$  induced orientational ordering of  $C_{70}$  relies on a rather weak  $C_{70}$ -HOPG interaction. If HOPG is substituted with another substrate which forms a strong directional bond with  $C_{70}$ , the  $C_{70}$  molecule may not be able to alter its orientation.

A challenging task is to grow a van der Waals solid consisting of alternating  $C_{60}$  and  $C_{70}$  layers. This is highly desirable in view of making new materials with tunable properties. One of the difficulties for growing such well-controlled multilayer structures is to achieve layer-by-layer growth. Under the standard growing conditions, we always observe the appearance of the second layer islands before the first layer is completed. The second layer islands subsequently affects the formation of the whole second layer. By experimenting with the deposition flux and the sample temperature, there is some possibility of finding an optimized condition for pure layer-by-layer epitaxy.

In summary, the ellipsoidal shape of  $C_{70}$  can make significant contributions to the structure of the  $C_{60}$ - $C_{70}$  interface. By choosing an orientation that lattice matches the close-packed  $C_{60}$  layer, a strain-free heterostructure can be obtained. This scheme allows the fabrication of lattice-matched  $C_{60}$ - $C_{70}$  multilayers. Giving up some degrees of rotational freedom leads to a reduced entropy of the  $C_{70}$  layer. This reduction in entropy is over compensated by the reduced interfacial energy. The phenomenon of orientational epitaxy discovered for the  $C_{60}$ - $C_{70}$  system is

expected to be operative for other systems involving particles with non-spherical symmetry, and scalable up to nano-particles or colloidal systems.<sup>21,43</sup>

**Methods.** Highly oriented pyrolytic graphite (purchased from Goodfellow, 99.99% purity) was used as the substrate. The HOPG sample was cleaned by annealing in ultra-high vacuum (UHV) at 475 K for 30 min to remove surface contamination just before deposition.  $C_{60}$  and  $C_{70}$  molecules (purchased from MER, 99.5% purity) were sublimed onto the HOPG substrate using home-built effusion cells. The effusion cells were degassed at 500 K for 5 min before sublimation. Then the  $C_{60}$  and  $C_{70}$  molecules were deposited on the surface with a rate of 0.12 and 0.10 ML/min, respectively. During deposition, the background pressure in the UHV system did not exceed  $10^{-9}$  mbar. STM imaging was performed with an Omicron UHV variable temperature STM using electrochemically etched tungsten tips. Images were collected in constant current mode with tunnelling current set at 0.1 nA and bias voltage in the range between +2.00 V and +2.58 V.

■ **Acknowledgment.** We thank the Chinese Scholarship Council for providing a studentship to Lu'an Guo.

#### ■ AUTHOR INFORMATION

\*Corresponding author

[Q.Guo@bham.ac.uk](mailto:Q.Guo@bham.ac.uk), Tel. +44 1214144657

#### ■ REFERENCES

- (1) Faist, J.; Cappasso, F.; Sivco, D. L.; Sirtori, C.; Hutchinson, A. L.; Cho, A. Y. *Science* **1994**, 264, 553-556.
- (2) Yan, R. S. *et al. Nature* **2018**, 555, 183-189.
- (3) Venables, J.; Spiller, G.; Hanbucken, M. *Rep. Prog. Phys.* **1984**, 47, 399-459.
- (4) Zhang, Z.; Lagally, M. G. *Science* **1997**, 276, 377-383.
- (5) Fu, D. Y. *et al. J. Am. Chem. Soc.* **2017**, 139, 9392-9400.
- (6) Lin, M. *et al. J. Am. Chem. Soc.* **2013**, 135, 13274-13277.
- (7) Jariwala, D.; Marks, T. J.; Hersam, M. C. *Nat. Mater.* **2017**, 16, 170.
- (8) Falcato, P.; *et al. Nat. Mater.* **2017**, 16, 342.
- (9) Eremtchenko, M.; Schaefer, J. A.; Tautz, F. S. *Nature* **2003**, 425, 602-605.
- (10) Nakayama, Y.; *et al. Appl. Mater. & Interface.* **2016**, 8, 13499-13505.
- (11) Ganapathy, R.; Buckley, M. R.; Gerbode, S. J.; Cohen, I. *Science* **2010**, 327, 445-448.
- (12) Babrys, P. A. *et al. Nano Lett.* **2018**, 18, 579-585.
- (13) Palmstrom, C. J. *Annu. Rev. Mater. Sci.* **1995**, 25, 389-415.
- (14) Xie, S.; Tu, L.; Han, Y.; Huang, L.; Kang, K.; Lao, K. U.; Poddar, R.; Park, C.; Muller, D. A.; DiStasio, R. A.; Park, J. *Science* **2018**, 359, 1131-1136.
- (15) Schlom, D. G.; *et al. MRS Bulletin* **2014**, 39, 118-130.
- (16) Wang, R.; Lange, F. R. L.; Cecchi, S.; Hanke, M.; Wuttig, M.; Calarco, R. *Adv. Func. Mater.* **2018**, 28, 1705901.
- (17) Koma, A. *Thin Solid Films* **1992**, 216, 72-76.
- (18) Gobbi, M.; Orgiu, E.; Samori, P. *Adv. Mater.* **2018**, 30, 1706103.
- (19) Richardson, J. J.; Cui, J.; Bjornmalm, M.; Braunger, J. A.; Ejima, H.; Caruso, F. *Chem. Rev.* **2016**, 116, 14828-14867.
- (20) Kleppmann, N.; Schreiber, F.; Klapp, S. H. L. *Phys. Rev. E.* **2017**, 95, 020801.
- (21) Damasceno, P.; Engel, M.; Glotzer, S. *Science* **2012**, 337, 453-457.

- (22) Meijer, J.-M.; Pal, A.; Ouhajji, S.; Lekkerkerker, H. N. W.; Philipse, A. P.; Petukhov, A. V. *Nat. Commun.* **2017**, DOI: 10.1038/ncomms14352.
- (23) Campoy-Quiles, M. *et al. Nat. Mater.* **2008**, 7, 158-164.
- (24) Schmidt-Hansberg, B. *et al. ACS Nano* **2011**, 5, 8579-8590.
- (25) Xie, Y.-C.; Tang, L.; Guo, Q. *Phys. Rev. Lett.* **2013**, 111, 186101.
- (26) Kaya, D.; Bao, D.-L.; Palmer, R. E.; Du, S.-X.; Guo, Q. *Nano Lett.* **2017**, 17, 6171-6176.
- (27) Xie, Y.-C.; Rokni Fard, M.; Kaya, D.; Bao, D.-L.; Palmer, R. E.; Du, S.-X.; Guo, Q. *J. Phys. Chem. C* **2016**, 120, 10975-10981.
- (28) Bommel, S.; Kleppmann, N.; Weber, C.; Spranger, H.; Schafer, P.; Novak, J.; Roth, S. V.; Schreiber, F.; Klap, S. H. L.; Kowarik. *Nat. Commun.* **2014**, DOI: 10.1038/ncomms6388.
- (29) Freund, S.; Hinaut, A.; Pawlak, R.; Liu, S.-X.; Decurtins, S.; Meyer, E.; Glatzel, T. *ACS Nano* **2016**, 10, 5782-5788.
- (30) Korner, M.; Loske, F.; Einax, M.; Kuhnle, A.; Reichling, M. Maass, P. *Phys. Rev. Lett.* **2011**, 107, 016101.
- (31) Zhang, X.; Tang, L.; Guo, Q. *J. Phys. Chem. C* **2010**, 114, 6433.
- (32) Li, H. I.; Pussi, K.; Hanna, K. J.; Wang, L. L.; Johnson, D. D.; Cheng, H. P.; Shin, H.; Curtarolo, S.; Moritz, W.; Smerdon, J.; McGrath, R.; Diehl, R. D. *Phys. Rev. Lett.* **2009**, 103, 056101.
- (33) Gardener, J. A.; Briggs, G. A. D.; Castell, M. R. *Phys. Rev. B.* **2009**, 80, 235434.
- (34) Altman, E. I.; Colton, R. J.; *Surf. Sci.* **1993**, 295, 13.
- (35) Tzeng, C. T.; Lo, W. S.; Yuh, J. Y.; Chu, R. Y.; Tsuei, K. D.; *Phys. Rev. B.* **2000**, 61, 2263.
- (36) Havlik, D.; Schranz, W. *Phase Transitions* **1999**, 67, 779-788.
- (37) Baba, M. S.; Narasimhan, T. S. L.; Balasubramanian, R.; Sivaraman, N.; Mathews, C. K. *J. Phys. Chem.* **1994**, 98, 1333-1340.
- (38) Rossel, F.; Pivetta, M.; Pathe, F.; Cavar, E.; Seitsonen, A. P.; Schneider, W.-D. *Phys. Rev. B* **2011**, 84, 075426.
- (39) Olyanich, D. A.; Mararov, V. V.; Utas, T. V.; Zotov, A. V.; Saranin, A. A. *Surf. Sci.* **2016**, 653, 138-142.
- (40) Dresselhaus, M. S.; Dresselhaus, G.; Eklund, P. C. *Science of Fullerenes and Carbon Nanotubes*. (Academic Press, New York, 1996).
- (41) Vaughan, G. B. M.; Heiney, P. A.; Cox, D. E.; Fischer, J. E.; McGhie, A. R.; Smith, A. Strongin, R. M.; Cichy, M. A.; Smith III, A. B. *Chem. Phys.* **1993**, 178, 599-613.
- (42) Donev, A.; Stillinger, F.; Chaikin, P. M.; Torquato, S. *Phys. Rev. Lett.* **2004**, 92, 255506.
- (43) Kang, C. J.; Honciuc, A. *ACS Nano* **2018**, 12, 3741-3750.

